



HHS Public Access

Author manuscript

Curr Pharm Biotechnol. Author manuscript; available in PMC 2017 March 14.

Published in final edited form as:

Curr Pharm Biotechnol. 2012 June ; 13(7): 1346–1359.

Experimental Methods and Transport Models for Drug Delivery across the Blood-Brain Barrier

Bingmei M Fu

Department of Biomedical Engineering, The City College of the City University of New York, 160 Convent Ave., New York, NY 10031 USA

Abstract

The blood-brain barrier (BBB) is a dynamic barrier essential for maintaining the micro-environment of the brain. Although the special anatomical features of the BBB determine its protective role for the central nervous system (CNS) from blood-born neurotoxins, however, the BBB extremely limits the therapeutic efficacy of drugs into the CNS, which greatly hinders the treatment of major brain diseases. This review summarized the unique structures of the BBB, described a variety of *in vivo* and *in vitro* experimental methods for determining the transport properties of the BBB, e.g., the permeability of the BBB to water, ions, and solutes including nutrients, therapeutic agents and drug carriers, and presented newly developed mathematical models which quantitatively correlate the anatomical structures of the BBB with its barrier functions. Finally, on the basis of the experimental observations and the quantitative models, several strategies for drug delivery through the BBB were proposed.

Keywords

Drug delivery; *in vivo* and *in vitro* blood-brain barrier models; paracellular pathway; permeability of the blood-brain barrier; transcellular pathway; transport models

1. Introduction

The most complicated organ in our body is the brain. It contains 100 billion neurons and 1 trillion glial cells (non-nerve supporting cells in the brain including astrocytes, oligodendrocytes, microglia, and ependymal cells). Along with a tremendous amount of blood vessels, these cells and surrounding extracellular matrix form a highly complex, though well organized 3-D interconnecting arrays. In order to perform its highly complicated tasks, the brain needs a substantial amount of energy to maintain electrical gradients across neuronal membranes and consequently requires a sufficient supply of oxygen and nutrients. Although it only accounts from 2% of the body weight, the brain uses 20% of the blood supply. The blood is delivered through a complex network of blood vessels that runs > 650 km and passes a surface area of $\sim 20 \text{ m}^2$. The mean distance between adjacent capillaries is $\sim 40 \mu\text{m}$, which allows almost instantaneous equilibration in the brain tissue surrounding the microvessels for small solutes such as glucose, amino acids, vitamins,

oxygen, etc. However, unlike peripheral microvessels in other organs where there is a relatively free small solute exchange between blood and tissue, the microvessels in the brain (cerebral microvessels) constrain the movement of molecules between blood and the brain tissue [1, 2]. This unique characteristic provides a natural defense against toxins circulating in the blood, which, on the other hand, prevents the delivery of therapeutic agents to the brain.

The vascular barrier system in the brain consists of the blood-brain barrier (BBB) and the blood-cerebrospinal fluid (CSF) barriers. There is another barrier, the brain-CSF barrier, between brain tissue and the CSF. [3]. The blood-brain barrier (BBB) is the name for the wall of the cerebral microvessels in the brain parenchyma. At the surface of the brain parenchyma, microvessels running in the pia mater are called pial microvessels, which are often used as in vivo models for studying the BBB permeability. Due to its unique structure that will be discussed in the next section, the BBB maintains very low permeability to water and solutes. In the middle of the brain parenchyma, there are ventricular cavities (ventricles) filled with CSF secreted by the epithelial cells of choroid plexus [4]. The choroid plexus is a highly vascular tissue with leaky, fenestrated capillaries covered with ependymal epithelium, which has relatively tight junctions. The multi-cell layer between the blood and the CSF in the choroid plexuses is called the blood-CSF barrier. Since the area of the BBB is about 1000 times that of the blood-CSF barrier, it is more important to circumvent the impermeability of the BBB for delivering drugs to the brain [5, 6]. The total surface area of the BBB constitutes by far the largest interface for blood-brain exchange, which is between 12 and 18 m² for the average human adult [7]. Unlike these two tight blood barriers, the interface between the CSF and brain tissue along the ependymal surface of the ventricles and that between pia mater and brain tissue, so called the brain-CSF barriers, are rather leaky, implying a possible route for drug delivery to the brain. The CSF is formed by the choroid plexuses of the ventricles, passes the ventricles to the subarachoid space over the pia mater, and finally absorbed to the venules in the dura mater through arachnoid microvilli and arachnoid granulations [8, 9].

1.1 The Blood-Brain Barrier

The blood-brain barrier (BBB) is a unique dynamic regulatory interface between the cerebral circulation and the brain tissue, and it is essential for maintaining the micro-environment within brain. No other body organ so absolutely depends on a constant internal micro-environment as does the brain. In brain, the extracellular concentrations of amino acids and ions such as Na⁺, K⁺, and Ca²⁺ must be retained in very narrow ranges [2]. If the brain is exposed to big chemical variations for these molecules, neurons would not function properly because some amino acids serve as neurotransmitters and certain ions modify the threshold for neuronal firing. The BBB also protects the central nervous system (CNS) from blood-borne neuroactive solutes, such as glutamate, glycine, norepinephrine, epinephrine, and peptide hormones [10], which can increase with physiological changes (e.g., diet and stress) and pathological changes (e.g., injury and diseases). In addition, the BBB plays a key role in facilitating the brain uptake of essential nutrients like glucose, hormones and vitamins, and larger molecules like insulin, leptin and iron transferring to sustain brain growth and metabolism [11].

The term “blood-brain barrier” was coined by Lewandowsky in 1900 while he demonstrated that neurotoxic agents affected brain function only when directly injected into the brain but not when injected into the systemic circulation [12]. Nevertheless, the first experimental observation of this vascular barrier between the cerebral circulation and the CNS should date back to the 1880s, when Paul Ehrlich discovered that certain water-soluble dyes, like trypan blue, after injected into the systemic circulation, were rapidly taken by all organs except the brain and spinal cord [13]. Ehrlich interpreted these observations as a lack of the affinity of the CNS for the dyes. However, subsequent experiments performed by Edwin Goldmann, an associate of Ehrlich, demonstrated that the same dyes, when injected directly into the CNS, stained all types of cells in the brain tissue but not any other tissues in the rest of the body [14]. It took additional 70 years until this barrier was firstly localized to cerebral microvascular endothelial cells by electron-microscopic studies performed by Reese and Karnovsky [15]. Although the concept of the BBB has continued to be refined over the past few decades, the recent understanding of the basic structure of the BBB is built on the general framework established by their studies in the late 1960s; more specifically, the BBB exists primarily as a selective diffusion barrier at the level of cerebral capillary endothelium.

The anatomical structure of the blood-brain barrier is shown in Figure 1b. For comparison, the cross-sectional view of a peripheral microvessel (a typical microvessel in non-brain organs) is also shown in Figure 1a. For both peripheral microvessels and the BBB, the circumference of the microvessel lumen is surrounded by endothelial cells, the opposing membranes of which are connected by tight junctions. At the luminal surface of the endothelial cell, there is a rather uniform fluffy glycocalyx layer [16–20]. This mucopolysaccharide structure is highly hydrated in electrolytic solution and contains large numbers of solid-bound fixed negative charges due to the polyanionic nature of its constituents abundant in glycoproteins, acidic oligosaccharides, terminal sialic acids, proteoglycan, and glycosaminoglycans aggregates [21]. Pericytes attach to the abluminal membrane of the endothelium at irregular intervals. In a peripheral microvessel, there is a loose and irregular basal lamina (or basement membrane) surrounding the pericytes. In contrast, in the BBB, pericytes and endothelial cells are ensheathed by a very uniform basement membrane of 20–40 nm thickness, which is composed of collagen type IV, heparin sulfate proteoglycans, laminin, fibronectin, and other extracellular matrix proteins [22]. The basal lamina is contiguous with the plasma membranes of astrocyte end-feet that wraps almost the entire abluminal surface of the endothelium [2].

In addition to the anatomical structures, the BBB differs from the peripheral microvessels in the following aspects. The mitochondrial content of the endothelial cells forming the BBB is greater than that of such cells in all non-neural tissues. It is suggested that this larger metabolic work capacity may be used to maintain the unique structural characteristics of the BBB, or/and by metabolic pumps that may require energy to maintain the differences in composition of the cerebral circulation and the brain tissue [23]. The BBB has high electrical resistance, much less fenestration, and more intensive junctions, which are responsible for restricting paracellular passage of water and polar solutes from the peripheral circulation entering into the CNS [24, 25]. Between adjacent endothelial membranes, there are junctional complexes which include adherens junctions (AJs), tight junctions (TJs), and possibly gap junctions [26]. The structure of the junction complexes between endothelial

cells is shown in Figure 2 [27, 28]. Both AJs and TJs act to restrict paracellular transport across the endothelium while gap junctions mediate intercellular communication. AJs are ubiquitous in the vasculature and their primary component is vascular endothelial (VE)-cadherin. They basically mediate the adhesion of endothelial cells to each other and contact inhibition during vascular growth and remodeling. Although disruption of AJs at the BBB can lead to increased permeability, TJ is the major junction that confers the low paracellular permeability and high electrical resistance [29]. The tight junction complex includes two classes of trans-membrane molecules: occludins and claudins. These trans-membrane proteins from adjacent endothelial cells interact with each other and form seals in the spaces between adjacent endothelial cells. The cytoplasmic tails of the trans-membrane proteins are linked to the actin cytoskeleton via a number of accessory proteins such as members of the zonula occludens family, ZO-1, ZO-2 and ZO-3.

A number of grafting and cell culture studies have suggested that the ability of cerebral endothelial cells to form the BBB is not intrinsic to these cells, but the cellular milieu of brain somehow induces the barrier property into the blood vessels. It is believed that all components of the BBB are essential for maintaining functionality and stability of the BBB. Pericytes seem to play a key role in angiogenesis, structural integrity, and maturation of cerebral microvessels [30]. The extracellular matrix of the basal lamina appear to serve as an anchor for the endothelial layer via interaction of laminin and other matrix proteins with endothelial integrin receptors [31]. It was suggested that astrocytes are critical in the development and/or maintenance of unique features of the BBB. Additionally, astrocytes may act as messengers to or in conjunction with neurons in the moment-to-moment regulation of the BBB permeability [30].

1.2 Transport Pathways across the Blood-Brain Barrier

The BBB endothelial cells differ from those in peripheral microvessels by more intensive tight junctions, sparse pinocytotic vesicular transport, and much less fenestrations. The transport of substances from the capillary blood into the brain tissue depends on the molecular size, lipid solubility, binding to specific transporters, and electrical charge [32]. Figure 3 summarizes the transport routes across the BBB [33]. Compared to the peripheral microvessel wall, the additional structure of the BBB and tighter endothelial junctions greatly restrict hydrophilic molecules transport through the gaps between the cells, i.e., the paracellular pathway of the BBB, route A in Figure 3. In contrast, small hydrophobic molecules such as O₂ and CO₂ diffuse freely across plasma membranes following their concentration gradients, i.e., the transcellular lipophilic diffusion pathway, route C in Figure 3. The BBB permeability to most molecules can be estimated on the basis of their octanol/water partition coefficients [34]. For example, diphenhydramine (Benadryl), which has a high partition coefficient, can easily cross the BBB, whereas water-soluble loratadine (Claritin) is not able to penetrate the BBB and has little effect on the CNS [35].

However, the octanol/water partition coefficients do not completely reflect BBB permeability to solutes. Some solutes with low partition coefficients that easily enter into the CNS generally cross the BBB by active or facilitated transport mechanisms, which rely on ion channels, specific transporters, energy-dependent pumps, and a limited amount of

receptor-mediated transcytosis. Glucose, amino acids, and small intermediate metabolites, for example, are ushered into brain tissue via facilitated transport mediated by specific transport proteins (route B in Figure 3), whereas larger molecules, such as insulin, transferrin, low density lipoprotein and other plasma proteins, are carried across the BBB via receptor-mediated (route D) or adsorptive transcytosis (route E). Some small molecules with high octanol/water partition coefficients are observed to poorly penetrate the BBB. Recent studies suggested that these molecules are actively pumped back into blood by efflux systems (route F in Figure 3). These efflux systems greatly limit drug delivery across the BBB. For instance, P-glycoprotein (P-gp), which is a member of the adenosine triphosphate-binding cassette family of exporters, has been demonstrated to be a potent energy-dependent transporter. P-gp contributes greatly to the efflux of xenobiotics from brain to blood and has increasingly been recognized as having a protective role and being responsible for impeding the delivery of therapeutic agents [36]. The organic anion transporters and glutathione-dependent multidrug resistance-associated proteins (MRP) also contribute to the efflux of organic anions from the CNS, and many drugs with the BBB permeabilities that are lower than predicted are the substrates for these efflux proteins [2, 28, 33, 37]. While the brain endothelium is the major barrier interface, the transport activity of the surrounding pericytes [38], basement membrane and astrocyte foot processes (Figure 1b) [39] also contribute to the BBB barrier function under physiological conditions, and may act as a substitute defense if the primary barrier at the endothelium is compromised [40].

2. Drug Delivery through the Blood-Brain Barrier

The endothelial cells lining microvessel walls provide the rate-limiting barrier to extravasation of plasma components of all sizes from electrolytes to proteins. In addition to the tight junction of the microvessel endothelium, there is a uniform and narrow matrix-like basement membrane layer (20–40nm) sandwiched between the vessel wall and the astrocyte processes ensheathing the cerebral microvessel (Figure 1b). To develop effective and efficient methods for drug delivery to the brain through the BBB with the largest contact area with brain tissue, we need to understand the mechanism by which these structural components, as well as transporters, receptors, efflux pumps and other components at the endothelium and astrocyte foot processes control the permeability of the BBB to water and solutes.

2.1 Permeability of the Blood-Brain Barrier

The same as a peripheral microvessel, the wall of the BBB can be viewed as a membrane. The membrane transport properties are often described by Kedem-Katchalsky equations derived from the theory of irreversible thermodynamics [41],

$$\begin{aligned} J_s &= PRT\Delta C + (1 - \sigma_f)CJ_v \\ J_v &= L_p(\Delta p - \sigma_d RT\Delta C) \end{aligned}$$

where J_s and J_v are the solute and volumetric fluxes; C and p are the concentration and pressure difference across the membrane. L_p , the hydraulic conductivity, describes the

membrane permeability to water. P , the diffusive permeability, describes the permeability to solutes. σ_f is the solvent drag or ultrafiltration coefficient that describes the retardation of solutes due to membrane restriction, and σ_d , the reflection coefficient, describes the selectivity of membrane to solutes. In many transport processes, σ_f is equal to σ_d and thus we often use σ , the reflection coefficient, to represent both of them. These three coefficients can be determined experimentally and theoretically. In addition to these quantitative coefficients, there are other less quantitative permeability indicators for the BBB, e.g., brain uptake index (BUI), and brain efflux index (BEI) [2]. In the following sections, *in vivo* and *in vitro* experiments for determining permeability of the BBB are introduced, as well as the mathematical models.

2.2 Determination of the Blood-Brain Barrier Permeability *in vivo* and *ex vivo*

Several *in vivo* and *ex vivo* rat models have been used for the study of the transport across the BBB, including pharmacokinetic methods [42–44], intracerebral microdialysis [45], positron emission tomography (PET) [46], magnetic resonance imaging (MRI) [47], the intravital microscopy study [48], occluding single microvessel measurement [49], and single microvessel fluorescence imaging method [50].

Pharmacokinetic methods are used to evaluate the delivery of a molecule from the systemic circulation into the brain, in which the amount of solute delivered to the brain can be expressed by percentage of injected dose delivered per gram of the brain. Generally, a small volume of buffered Ringer's solution containing the radio-labeled compound of interest and a radio-labeled diffusible reference compound as an internal standard (such as ^3H -water) is injected into the common carotid artery, or the internal carotid artery, or the venule depending on different techniques. Then, the animal is sacrificed 5–15s after injection, and the brain tissue and the injection solution are analyzed to calculate the brain uptake index (BUI), which is the ratio of radio-labeled test compound/ ^3H reference in the brain, divided by the ratio of radio-labeled test compound/ ^3H reference in the injection mixture [2]. Another permeability indicator, brain efflux index (BEI), can also be determined using this method. $\text{BEI} = (\text{amount of test compound injected into the brain} - \text{amount of test compound remaining in the brain}) / \text{amount of test compound injected into the brain}$. The assumptions of these models are: 1) the reference compound is freely diffusible across the BBB; 2) the drug does not back-diffuse from the brain to blood; and 3) no metabolism of the compounds occurs before decapitation. The advantage of these pharmacokinetic methods is fast and many compounds can be assessed in a short time, which is ideal in the high-throughput setting. The major disadvantages are: 1) brain extraction only occurs over a limited time, making it difficult to accurately determine the brain uptake index [2]; 2) the driving force for the transport is unknown.

Intracerebral microdialysis involves direct sampling of brain interstitial fluid by a dialysis fiber implanted into the brain parenchyma. The concentration of compound that has permeated into the brain following oral, intravenous or subcutaneous administration can be monitored over time within the same animal. Any drug that enters the brain interstitial fluid will permeate into the physiological solution within the probe, and the solution may be subsequently assayed by an appropriate technique. The major advantage of this technique is

that it provides pharmacokinetic profiles of drugs in the brain without killing animals at different time points. One limitation of this technique is that it greatly relies on and limited by the sensitivity of the assay technique [45], since the solute concentrations may be extremely low in the dialysate. Another major disadvantage is that insertion of the probe can result in chronic BBB disruption.

More recently, various imaging techniques, including positron emission tomography (PET) and magnetic resonance imaging (MRI) have been used to determine BBB permeability in humans. PET is a non-invasive tracer technique used to quantify the BBB extravasation. Magnetic resonance imaging (MRI) is also non-invasive techniques, but it is more qualitative than quantitative. The major disadvantages for these techniques include their inherent costs, labor intensity, relatively low resolution (100 μ m to 1mm per pixel) and inability to differentiate between parent compound and metabolites [50, 51].

All of the above-mentioned methods only measure certain indexes of relative permeability for the drug uptake to brain since they cannot determine the driving force for the efflux. Because it is hard to measure the BBB permeability in brain parenchyma, the microvessels in pia dura at the surface of brain are often used in *in vivo* BBB permeability study. Although pial microvessels do not have the entire ensheathment of astrocytes as those cerebral microvessels in the parenchyma, the pial and cerebral microvessels appear to have many morphophysiological properties in common. These include ultrastructural characteristics, permeability of cell junctions to electron dense tracers, trans-endothelium electrical resistance, and molecular properties of endothelium. For these reasons, pial microvessels are often used in the BBB permeability studies [52].

Gaber *et al.* [48] suggested a method to measure clearance or leakage of drug out of the pial microvessels rather than 'true' permeability of the microvessels to solute. Again, this method cannot determine the driving force, the concentration difference of the test solute across the BBB. The occluding single microvessel measurement is done directly on one single exposed pial microvessel after the frontal craniotomy removing a small section of skull and the dura mater [49]. This method has well-controlled conditions including known concentration difference across the microvessel wall. However, recent study suggests that the exposed rat pial microvessels become leaky to both small and large molecules within 20–60 minutes following the craniotomy and the permeability of the exposed microvessels rises sharply after 160 minutes [53].

To quantify the permeability of intact rat pial microvesels and overcome the above mentioned disadvantages, Yuan et al. [50] developed a non-invasive method, without exposing the cortex, to measure the solute permeability (P) of post-capillary venules on rat pia mater to various sized solutes. The pial microvessels were observed by a high numerical aperture objective lens through a section of frontoparietal bones thinned with a micro-grinder (revised surgical method from [49]). P was measured on individual pial venular microvessels with the perfused fluorescence tracer solution through the carotid artery by using highly sensitive quantitative fluorescence microscope imaging method. The major procedures are shown in Figures 4, 5. Their results indicate that the solute permeability of rat pial microvessels is about an order of magnitude lower than that of rat mesenteric

microvessels, from 1/11 for a small solute, sodium fluorescein, to 1/6 for a large solute, albumin or dextran 70k. The permeability of rat mesenteric microvessels to these solutes was measured by Fu and Shen [54]. With the development of multiphoton microscopy, the solute permeability of cerebral microvessels in the parenchyma can be quantified by using longer wavelength lasers for the deeper penetration.

2.3 *In vitro* Blood-Brain Barrier Models

The development of *in vitro* models for the BBB has enabled the study of transport phenomena at the molecular and cellular levels. The aim of such *in vitro* BBB models is to functionally resemble as many as possible the unique characteristics of the BBB. Compared with *in vivo* animal models, the *in vitro* models are relatively accessible, flexible, reproducible and abundantly available. Previous investigations showed that the permeability of the *in vitro* BBB models to various compounds such as sucrose, retinoic acid, retinol, haloperidol, caffeine, and mannitol was comparable to the permeability data obtained from *in vivo* models [55].

To characterize the transport properties of *in vitro* BBB models, the solute permeability of the *in vitro* BBB was determined by measuring the flux of the selected tracer. The most commonly used cell culture substrate consists of a porous membrane support submerged in the culture medium (Transwell apparatus). The Transwell system is characterized by a horizontal side-by-side or vertical diffusion system. During the experiment, the flux of tracers into the abluminal compartment of the Transwell system is recorded as a function of the time and the solute permeability is calculated from the slope of the flux. The tracers used in the transport experiments are labeled by a fluorescent dye or isotope whose intensity can be measured quantitatively. Another index, Trans-endothelial Electrical Resistance (TEER), or the ionic conductance of the monolayer, is also a measurement of the “tightness” of the *in vitro* BBB models.

So far, two major types of *in vitro* BBB models have been developed: endothelial cell monolayer and coculture of endothelial cells with glial cells (the non-nerve cells in the brain). The cells for these models are basically obtained from primary/sub-passaged or immortalized cell cultures. The origins of the cells are also very diverse: human, primate, bovine, porcine, rodent and murine species.

The brain capillary endothelial cells (BCEC) have been used to establish tissue culture systems ever since the technique of culturing highly purified populations of microvascular cells became available in the early 1980s. The first endothelial monolayers were established using BCEC grown on culture dishes, microcarriers (e.g., dextran beads), and various kinds of filters, including nylon mesh and polycarbonate. These cultured BCEC cells keep their endothelial phenotypes and provides a simple model for study the permeability of the BBB. For instance, they express angiotensin converting enzyme, von Willebrand factor, and internalize accetylated low-density lipoprotein. However, they were reported to lose many BBB-specific features they possessed *in vivo*. For instance, they are lack of specific brain endothelial markers γ -glutamyl transpeptidas, marker enzyme alkaline phosphatase [56], and glucose transporter system [57]. Moreover, the permeability of the BCEC monolayer to sucrose was reported to be from 10^{-4} to 10^{-5} cm/s compared with 10^{-6} cm/s *in vivo*. The

TEER for endothelial monolayer was also found to be pretty low, from 20 to 1,400 $\Omega\cdot\text{cm}^2$, compared with more than 2,000 $\Omega\cdot\text{cm}^2$ *in vivo*. So the BCEC monolayer alone is not a well-characterized model for the BBB. The major reason for this may be the lack of *in situ* environment and brain-derived signals.

In human body, the BBB are almost completely ensheathed by surrounding tissue, mostly astrocyte foot processes. Experimental results from electron microscopic techniques show that astrocytes do have significant effects on the formation of the unique BBB phenotype of brain endothelial cells [58, 59]. They induce formation of the tight junctions between endothelial cells and increase paracellular integrity of the BBB. To better mimic the *in vivo* BBB, a model with coculture of BCEC and astrocyte was developed. This coculture model was characterized on the basis of specific cell-type properties and specific BBB properties by electron microscopic evaluation and immunohistochemistry methods [60]. The results showed that BCEC displayed (1) characteristic endothelial cell morphology; (2) expression of endothelial cell markers (i.e., CD51, CD62P, CD71 and cadherin 5); (3) tight junction formation between the cells; (4) expression of typical barrier marker γ -glutamyl-transpeptidase (γ -GTP) and P-glycoprotein (Pgp) and transferrin receptor. Astrocytes displayed characteristic astrocyte morphology and expressed glial fibrillary acidic protein (GFAP). Transmission electron microscopy showed evidence of tight junction formation between the endothelial cells and few pinocytotic vesicles. A 15-fold increase in γ -glutamyl transpeptidase activity was measured in the endothelial cells cocultured with astrocytes [61]. The permeability of the coculture system to several tracers was reported to be lower than the endothelial monolayer. These results indicate that the coculture system is a better model to study the transport across the BBB.

Primary brain capillary endothelial cells have the closest resemblance to the BBB phenotype *in vivo*, and exhibit excellent characteristics of the BBB at early passages [51]. They, however, have inherent disadvantages such as being extremely time consuming and costly to generate, being easily contaminated by other neurovascular unit cells, losing their BBB characteristics over passages, and requiring high technical skills for extraction from brain tissue [62, 63]. An immortalized mouse brain endothelial cell line, bEnd3, has recently been under investigation for *in vitro* BBB models because of its numerous advantages over primary cell culture: the ability to maintain BBB characteristics over many passages, easy growth and low cost, formation of functional barriers and amenability to numerous molecular interventions [63–67]. Previous RT-PCR analysis showed that bEnd3 cells express the tight junction proteins ZO-1, ZO-2, occludin and claudin-5, and junctional adhesion molecules [63, 68]. They also maintained functionality of the sodium- and insulin-dependent stereospecific facilitative transporter GLUT-1 and the P-glycoprotein efflux mechanism (Omidi et al. 2003), formed fairly tight barriers to radiolabeled sucrose, and responded like primary cultures to disrupting stimuli [63].

To characterize the transport properties of *in vitro* BBB models, Malina et al. [69] and others [70–78] measured the diffusive permeability of endothelial cell monolayer and coculture of endothelial cells with astrocytes to fluorescence or isotope labeled tracers, e.g., sucrose, insulin, and mannitol. Sahagun et al. [79] reported the ratio between abluminal concentration and luminal concentration of different-sized dextrans (4k, 10k, 20k, 40k, 70k, and 150k)

across mouse brain endothelial cells. Gaillard and de Boer [60] measured the permeability of sodium fluorescein and FITC-labeled Dextran 4k across a coculture of calf brain capillary endothelial cells with rat astrocytes. Many investigators have measured the transendothelial electrical resistance (TER) of brain endothelial monolayers and cocultures as an indicator of ion permeability [80–83].

To seek for *in vitro* BBB models that are more accessible than animals for investigating drug transport across the BBB, Li et al. [84] characterized the junction protein expression and quantified the TER and permeability to water (L_p) and solutes (P) of four *in vitro* BBB models: bEnd3 monoculture, bEnd3 coculture with astrocytes, coculture with two BM substitutes: collagen type I and IV mixture, and Matrigel. Collagen type IV network is the basic framework of native BM [85, 86] and Matrigel is a soluble and sterile extract of BM derived from the EHS tumor, which has been widely used as a reconstituted BM in studying cell morphogenesis, differentiation and growth [87]. Their results show that L_p and P of the endothelial monoculture and coculture models are not different from each other. Compared with *in vivo* permeability data from rat pial microvessels, P of the endothelial monoculture and coculture models are not significantly different from *in vivo* data for Dextran 70K, but they are 2–4 times higher for small solutes TAMRA and Dextran 10K. This suggests that the endothelial monoculture and all of the coculture models are fairly good models for studying the transport of relatively large solutes (drugs or drug carriers) across the BBB.

2.4 Transport Models for the Paracellular Pathway of the Blood-Brain Barrier

Transport across the BBB include both paracellular and transcellular pathways [88]. While large molecules cross the BBB through transcellular pathways, water and small hydrophilic solutes cross the BBB through the paracellular pathway [25]. The paracellular pathway of the BBB is formed by the endothelial surface glycocalyx, tight junction openings, the BM filled with extracellular matrix and the openings between adjacent astrocyte foot processes (Figure 1b). In addition to the endothelial tight junctions, the BM and the astrocyte foot processes provide a significant resistance to water and solute transport across the BBB.

The breakdown of the BBB and increased permeability are widely observed in many brain diseases such as stroke, traumatic head injury, brain edema, Alzheimer's disease, AIDS, brain cancer, meningitis, et al. [89–95]. Although numerous biochemical factors are found to be responsible for the breakdown of the BBB in disease, the quantitative understanding of how these factors affect the structural components of the BBB to induce BBB leakage is poor. On the other hand, to design therapeutic drugs with better transport properties across the BBB relies greatly on this understanding. Therefore, it is important to investigate how the structural components in the paracellular pathway of the BBB affect its permeability to water and solutes through mathematical modeling.

Extended from a previous three-dimensional model for studying the transport across the peripheral microvessel wall with endothelium only [96, 97], Li et al. [40] developed a new model for the transport across the BBB, which included the BM and wrapping astrocyte foot processes. The simplified model geometry is shown in Figure 6. This is the enlarged view for the part near tight junction shown in Figure 1b. At the luminal side, there is an endothelial surface glycocalyx layer (SGL) with a thickness of L_f from 100–400 nm under

normal physiological conditions [16, 17, 19, 98]. Between adjacent endothelial cells, there is an inter-endothelial cleft with a length of $L \sim 500$ nm and a width of $2B \sim 20$ nm [98, 99]. In the inter-endothelial cleft, there is a L_{jun} (~ 10 nm) thick junction strand with a continuous slit-like opening of width $2B_s$, which varies depending on the location of the cerebral microvessels (from ~ 1 to 10 nm). The distance between the junction strand and luminal front of the cleft is L_1 . At the tissue side of the cleft, a BM separates the endothelium and the astrocyte foot processes. The thickness of the BM is $2L_b$ (20 – 40 nm) and the length of the astrocyte foot processes is $2W_a$ (~ 5000 nm). Between adjacent astrocyte foot processes, there is a cleft with length L_a (~ 1000 nm) and width $2B_a$ (20 – 2000 nm). The anatomic parameters for the BBB structural components were obtained from the electron microscopy studies in the literature.

Unlike the peripheral microvessel wall, the endothelium of the BBB has negligible large discontinuous breaks in the junction strand of the inter-endothelial cleft and the small slit in the junction strand is assumed continuous [25]. As a result, the cross-sectional BBB geometry is the same along the axial direction (y direction in Figure 6) and thus the model could be simplified to 2-D (in x, z plane). It could be further simplified to a unidirectional flow in each region due to very narrow clefts and the BM. In addition, the curvatures of the BM and the endothelium can be neglected because their widths are much smaller than the diameter of the microvessel. The fluid flow in the cleft regions of the BBB were approximated by the Poiseuille flow while those in the endothelial SGL and BM by the Darcy and Brinkman flows, respectively. Diffusion equations in each region were solved for the solute transport. After solving for the pressure, water velocity, and solute concentration profiles, the hydraulic conductivity L_p and solute permeability P can be calculated.

Figure 7a shows the model predictions for L_p as a function of tight junction opening B_s when the BM has different fiber densities. K_b is Darcy permeability in the BM. When the fiber density in the BM is the same as that in the SGL, $K_b = 3.16 \text{ cm}^2$. The green line in Figure 7a shows the case of peripheral microvessels with only endothelium. When B_s increases from 0.5 nm to 2 nm , L_p will increase by ~ 20 -fold. In contrast, when the endothelium is wrapped by the BM and the astrocytes as for the BBB, increase in B_s from 0.5 nm to 2 nm only induces 5-fold increase in L_p when the fiber density in the BM is the same as that in the SGL (dash-dot-dash line). If the fiber density in the BM is 10 times of that in the SGL, the increase is only 1.6-fold in L_p (solid line), while if the fiber density in the BM is $1/10$ of that in the SGL, the increase is 12-fold in L_p (dashed line). Even at a large B_s of 5 nm , when the BM is filled with the same density fibers as in the SGL, the BBB permeability is only 17% of that of endothelium only. This percentage can be as low as 2% if the fiber density in the BM is 10 times of that in the SGL. Figure 7b shows the model predictions for L_p as a function of the endothelial SGL thickness L_f . The green line is for the case of endothelium only while the solid line for that of the BBB. We can see the decrease in L_f from 400 to 0 nm increases L_p by 3-fold in the case of endothelium only, while in the case of the BBB, the increase is only 25% in L_p with the protection of the BM and the astrocytes. Similar results are predicted for the solute permeability (Li et al., 2010). These results indicate that the BM and astrocytes of the BBB provide a great protection to the CNS under both physiological and pathological conditions. However, on the other hand, these unique structures also impede the drug delivery to the brain through the BBB. Most recently,

an electro-diffusion model for the blood-brain barrier to the charged molecules was developed to take into consideration of the effect of charges in the SGL and BM on the solute transport across the BBB [100].

2.5 Strategies for Drug Delivery through the Blood-Brain Barrier

A large number of people in the world are now suffering from CNS diseases. The total number of patients with CNS diseases is reported to be larger than that with cardiovascular diseases [5]. While the BBB serves as a natural defense that safeguards the brain against the invasion of various circulating toxins and infected cells, it also provides a significant impediment toward the delivery of diagnostic and therapeutic agents to the brain via the systemic route. Essentially almost 100% of large-molecule drugs, including peptides, recombinant proteins, monoclonal antibodies, RNA interference (RNAi)-based drugs and gene therapies, and more than 98% of small-molecule cannot penetrate the brain microvessel wall by themselves [5].

Various methods such as intracerebral implantation, microdialysis, convection-enhanced distribution (CED), osmotic shock, and chemical modification of the BBB have been developed for delivering drugs into the brain. However, the applications of these methods are limited and they can only partially keep with the demands of modern therapies. For instance, the efficiency of intracerebral implantation, microdialysis and CED methods are low since their major transport mechanisms are diffusion and convection of interstitial fluid. The penetration distances of drugs delivered by the first two methods are reported to be less than 1mm with simple diffusion [101]. CED has been shown in laboratory experiments to deliver high molecular weight proteins 2 cm from the injection site in the brain parenchyma after 2 h of continuous infusion [102]. However, the success of CED relies on precise placement of the catheters and other infusion parameters for delivery into the correct location in the brain parenchyma. For effective treatment of the CNS diseases, therapeutic agents have to reach the specific regions of the brain at an adequate amount. As discussed earlier, due to the abundance and the largest contact area of the BBB for blood-brain exchange, it is more reasonable to develop strategies for drug delivery through the BBB.

As shown in Figure 3, we can directly deliver therapeutic agents through paracellular pathway (route A), lipophilic diffusion pathway (route C), or through transporters at the BBB by closely mimicking their substrates (route B), or mount the drugs on the ligands of the specific receptors expressed at the BBB (e.g., low density lipoprotein receptor related protein) for transcytosis (Trojan horse approach or receptor-mediated transcytosis, RMT, route D), as well as using cationized proteins, peptides and nanoparticle carriers for adsorptive mediated transcytosis (AMT, route E). The following summarizes the delivery strategies through these routes respectively.

2.5.1. Delivery through paracellular pathway (route A)—To increase the hydrophilic drug delivery from the blood to the brain tissue, we can transiently open the barriers in the paracellular pathway of the BBB, e.g. the cleft opening ($2B$ in Figure 6), the tight junction opening ($2B_s$), the BM width ($2L_b$), or degrade the fiber matrix in the endothelial surface glycocalyx and in the BM. Osmotic shock by intracarotid administration of a hyperosmotic

mannitol causes endothelial cells to shrink and increase 2B, 2B_s and 2L_b. Subsequent administration of drugs can increase their concentrations in the brain to a therapeutic level [103, 104]. Physical means such as application of electric and magnetic fields can increase the drug brain uptake. Focused ultrasound, guided by MRI, combined with microbubbles injected into the blood stream has been shown to disrupt the BBB and increase the distribution of Herceptin in brain tissue by 50% in mice [105–107]. Application of inflammatory agents such as bradykinin-analogue can open the tight junction of the BBB and increase the drug transport to the brain [108, 109]. However, these approaches are relatively costly and non-patient friendly. They may also enhance tumor dissemination after BBB disruption and damage the neurons by allowing the passage of unwanted blood components into the brain [110].

2.5.2. Delivery through lipophilic diffusion pathway (route C)—Some molecules, e.g., alcohol, nicotine and benzodiazepine, can freely enter the brain through route C in Figure 3. Their ability to passively (diffusion by concentration differences across the cell membrane) cross the BBB depends on the molecular weight (less than 500 D), charge (low hydrogen bonding capabilities) and lipophilicity [111]. Therefore, if we can modify the drugs through medicinal chemistry, e.g., reduce the relative number of polar groups, or incorporate them with a lipid carrier, we can enhance their brain uptake [2, 112]. Modification of antioxidants with pyrrolopyrimidines increases their ability to access target cells in the CNS [113]. Covalently attaching 1-methyl-1,4-dihydronicotinate to a hydroxymethyl group can enhance the delivery of ganciclovir (Cytovene, an antiviral medication) to the brain [114, 115]. However, the modification which helps for the drug delivery to the brain often results in loss of the therapeutic function of a drug. In addition, increase of lipophilicity of a drug can result in making it a substrate for the efflux pump P-glycoprotein (route F in Figure 3) [110].

2.5.3. Delivery through transporter-mediated pathway (route B)—The brain requires tremendous amount of essential substances for survival and function, e.g., glucose, insulin, hormones, low density lipoprotein (LDL), etc. These nutrients and substances are transported into the brain, not by paracellular or lipophilic diffusion pathway as described earlier, but by specific transporters or receptors at the BBB. Drugs can be modified to take advantages of the native BBB nutrient transporter systems, or by being conjugated to ligands that recognize receptors expressed at the BBB for the receptor-mediated transcytosis. This physiological approach is by far recognized as the most likely successful drug delivery method to the brain.

Peptides and small molecules may use specific transporters expressed on the luminal and basolateral sides of the endothelial cells to cross into the brain. So far, at least 8 different nutrient transporters have been identified to transport a group of nutrients with similar structures. Drugs can be modified to closely mimic the endogenous carrier substrates of these transporters and be transported through the specific transporter-mediated transcytosis. Dopamine can be used to treat Parkinson's disease, but itself is non-brain penetrant. Instead, dopamine's metabolic precursor, L-Dopa, if delivered by a neutral amino acid carrier through its transporter at the BBB, shows a clear clinical benefit on patients with

Parkinson's disease [116, 117]. To use a BBB transporter for drug delivery, several important factors must be considered: the kinetics and structural binding requirements of the transporter, therapeutic compound manipulation so that the compound binds but also remains active *in vivo*, and actual transport of the compound into the brain instead of just binding to the transporter [110].

2.5.4. Delivery through receptor-mediated pathway (route D)—Instead of by transporters, larger essential molecules are delivered into the brain by specific receptors highly expressed at the endothelial cells of the BBB. The receptor-mediated transcytosis (RMT) includes three steps: receptor-mediated endocytosis of the molecule at the luminal side of the endothelium (blood side), transport through the endothelial cytoplasm, and exocytosis of the molecule at the abluminal side of the endothelium (brain side). Although the exact mechanisms of RMT have not been well understood, drug delivery targeting three receptors, the insulin receptor, the transferrin receptor and the LDL receptor has been developed since the start of this century [116, 117]. More and more receptors have been targeted for the drug delivery since then [110]. This physiological approach is often called molecular Trojan horse since the therapeutic compounds are conjugated to the specific ligands or the antibodies, which can be recognized and delivered through transcytosis by the specific matching receptors at the endothelial cell membrane. In addition to molecular Trojan horses, drugs can be packaged to liposomes and other nanoparticles coated with targeting molecules such as antibodies to the specific receptors to improve the drug loading capacity.

Although the Trojan horses for the BBB drug delivery are very promising in delivering large peptides and recombinant proteins such as neurotrophins, enzymes and monoclonal antibodies (Pardridge, 2006), the traffic is limited by the number and carrying capacity of the receptors, as well as by the number of drug molecules that can attach to each antibody [118]. In addition, Gosk et al. [119] showed that using anti-transferrin mAb for drug delivery through the systemic administration, although the total amount of the drug in the brain is high, most of it stays associated with brain microvessel endothelial cells instead of in the brain parenchyma. Due to the high affinity of the antibodies, it is a challenge to dissociate from their specific receptors. Furthermore, widespread distribution of the receptors on peripheral organs would limit the specific delivery to the brain, and on the other hand, may induce additional toxicity.

2.5.5. Delivery through adsorptive-mediated pathway (route E)—Adsorptive-mediated transcytosis (AMT) involves endocytosis and exocytosis of charged substances by the endothelial cells of the BBB. Its mechanism is different from that of the RMT, which needs specific matching receptors and ligands. Kumagai et al. [120] observed that polycationic proteins such as protamine could not only bind to the endothelial cell surface but also penetrate the BBB. Mixing protamine, poly-L-lysine or other cationic molecules with proteins (e.g., albumin) largely increased the BBB permeability to these proteins. These findings can be explained by AMT triggered by electrostatic interactions between the positively charged proteins and negatively charged membrane regions at the brain endothelium. At normal physiological pH, the luminal surface of the cerebral endothelium

and the surrounding BM (see Figure 1b) carry negative charge [18, 121] and provide the necessary environment for delivering positively charged drugs and drug carriers. Recently, a quantitative *in vivo* animal study by Yuan et al. [122] found that the charge density of the endothelial surface glycocalyx and that of the BM in rat pial microvessels are ~30mEq/L. In another *in vitro* cell culture study, Yuan et al. [66] found the similar charge density on the surface of a cell monolayer of bEnd3, an immortalized mouse cerebral microvessel endothelial cell line.

To efficiently deliver a therapeutic protein or peptide across the BBB, the simplest way is to cationize the protein or peptide by amidation of its carboxylic acid groups, as well as glutamic and aspartic acid side chain groups with positively charged amines [123]. The degree of cationization of a protein or peptide may be critical for its pharmacokinetic fate. Cationization enhances the delivery while induces potential toxicity and immunogenicity of these proteins. PEGylation of cationized molecules can minimize the immunogenicity of these molecules. Positively charged cell-penetrating peptides (CPPs) are often used as the drug carriers for the brain delivery. Commonly used CPPs are penetratin, transportan, Syn-B and Tat [123]. Brain uptake of enkephalin analogue dalargin was enhanced several hundred folds after carried by the CPPs [124]. Decoration of CPPs on the surface of liposome and biopolymer-based nanoparticles containing drugs have shown to promote their uptake by the brain and entrance to the cytoplasm of neurons [125]. The drawbacks through AMT are lack of tissue selectivity although the BBB may contain higher concentrations of negative charges than other tissues, and possible disruption of the BBB and binding of polycationic substances to the negatively charged plasma proteins and other anionic sites resulting in toxicity [126].

Acknowledgments

The author would like to thank the funding support from NSF CBET-0754158, NIH SC1 CA153325, U54CA137788 and R01HL094889.

4. Bibliography

1. Abbott, NJ. Physiology and Pharmacology of the Blood-Brain Barrier. Springer; Heidelberg: 1992. Comparative physiology of the blood-brain barrier.
2. Pardridge WM. CNS drug design based on principles of blood-brain barrier transport. J Neurochem. 1998; 70:1781. [PubMed: 9572261]
3. Abbott NJ. Evidence for bulk flow of brain interstitial fluid: significance for physiology and pathology. Neurosci Int. 2004; 45:545.
4. Brown PD, Davies SL, Speake T, Millar ID. Molecular mechanisms of cerebrospinal fluid production. Neurosci. 2004; 129:957.
5. Pardridge, WM. Introduction to the Blood-Brain Barrier: Methodology, biology and Pathology. Cambridge University Press; Cambridge: 2006.
6. Pardridge WM. Drug targeting to the brain. Pharm Res. 2007; 24:1733. [PubMed: 17554607]
7. Nag, S., Begley, DJ. Pathology and Genetics. Cerebrovascular Diseases. ISN Neuropath. Press; Basel: 2005. Blood-brain barrier, exchange of metabolites and gases.
8. Culter RW, Page L, Galicich J, Watters GV. Formation and absorption of cerebrospinal fluid in man. Brain. 1968; 91:707. [PubMed: 5304069]
9. Redzic ZB, Segal MB. Adv Drug Del Rev. 2004; 56:1695.

10. Smith QR. Transport of glutamate and other amino acids at the blood-brain barrier. *J Nutr.* 2000; 130:1016.
11. Zhang Y, Pardridge WM. Rapid transferrin efflux from brain to blood across the blood-brain barrier. *J Neurochem.* 2001; 76:1597. [PubMed: 11238745]
12. Lewandowsky M. Zur lehre von der cerebrospinalflussigkeit. *Z Klin Med.* 1900; 40:480.
13. Ehrlich, P. Das sauerstoffbedurfnis des organismus. Hireschwald; Berlin: 1885.
14. Goldmann E. Vitalfärbung am zentralnervensystem. *Abhandl Kongil preuss Akad Wiss.* 1913; 1:1.
15. Reese TS, Karnovsky MJ. Fine structural localization of a blood-brain barrier to exogenous peroxidase. *J Cell Biol.* 1967; 34(1):207. [PubMed: 6033532]
16. Adamson RH, Clough G. Plasma proteins modify the endothelial cell glycocalyx of frog mesenteric microvessels. *J Physiol.* 1992; 445:473. [PubMed: 1501143]
17. Squire JM, Chew M, Nneji G, Neal C, Barry J, Michel CC. Quasi-periodic substructure in the microvessel endothelial glycocalyx: A possible explanation for molecular filtering? *Journal of Structural Biology.* 2001; 136(3):239. [PubMed: 12051903]
18. Ueno M, Sakamoto H, Liao YJ, Onodera M, Huang CL, Miyanaka H, Nakagawa T. Blood-brain barrier disruption in the hypothalamus of young adult spontaneously hypertensive rats. *Histochem Cell Biol.* 2004; 122(2):131. [PubMed: 15258771]
19. Vink H, Duling BR. Identification of distinct luminal domains for macromolecules, erythrocytes, and leukocytes within mammalian capillaries. *Circulation Research.* 1996; 79(3):581. [PubMed: 8781491]
20. Henry CB, Duling BR. Permeation of the luminal capillary glycocalyx is determined by hyaluronan. *American Journal of Physiology-Heart and Circulatory Physiology.* 1999; 277(2):H508.
21. Tarbell JM, Pahakis MY. Mechanotransduction and the glycocalyx. *Journal of Internal Medicine.* 2006; 259(4):339. [PubMed: 16594902]
22. Farkas E, Luiten PG. Cerebral microvascular pathology in aging and Alzheimer's disease. *Progress in Neurobiology.* 2001; 64(6):575. [PubMed: 11311463]
23. Oldendorf WH, Cornford ME, Brown WJ. The large apparent work capability of the blood-brain barrier: a study of the mitochondrial content of capillary endothelial cells in brain and other tissues of the rat. *Ann Neurol.* 1977; 1:409. [PubMed: 617259]
24. Butt AM, Jones HC, Abbott NJ. Electrical resistance across the blood-brain barrier in anaesthetized rats: a developmental study. *J Physiol.* 1990; 429:47. [PubMed: 2277354]
25. Hawkins BT, Davis TP. The blood-brain barrier/neurovascular unit in health and disease. *Pharmacol Rev.* 2005; 57:173. [PubMed: 15914466]
26. Simard M, Arcuino G, Takano T, Liu QS, Nedergaard M. Signaling at the gliovascular interface. *Journal of Neuroscience.* 2003; 23(27):9254. [PubMed: 14534260]
27. Kim JH, Park JA, Lee SW, Kim WJ, Yu YS, Kim KW. Blood-neural barrier: Intercellular communication at glio-vascular interface. *Journal of Biochemistry and Molecular Biology.* 2006; 39(4):339. [PubMed: 16889675]
28. Abbott NJ, Patabendige AK, Dolman DE, Yusof SR, Begley DJ. Structure and function of the blood-brain barrier. *Neurobiology of Disease.* 2010; 37:13.
29. Romero IA, Radewicz K, Jubin E, Michel CC, Greenwood J, Couraud PO, Adamson P. Changes in cytoskeletal and tight junctional proteins correlate with decreased permeability induced by dexamethasone in cultured rat brain endothelial cells. *Neuroscience Letters.* 2003; 344(2):112. [PubMed: 12782340]
30. Ballabh P, Braun A, Nedergaard M. The blood-brain barrier: an overview: structure, regulation, and clinical implications. *Neurobiol Dis.* 2004; 16:1. [PubMed: 15207256]
31. Hynes RO. Integrins: versatility, modulation, and signaling in cell adhesion. *Cell.* 1992; 69:11. [PubMed: 1555235]
32. Moody DM. The blood-brain barrier and blood-cerebral spinal fluid barrier. *Semin Cardiothorac Vasc Anesth.* 2006; 10(2):128. [PubMed: 16959739]
33. Neuwelt EA. Mechanisms of disease: the blood-brain barrier. *Neurosurgery.* 2004; 54(1):131. [PubMed: 14683550]

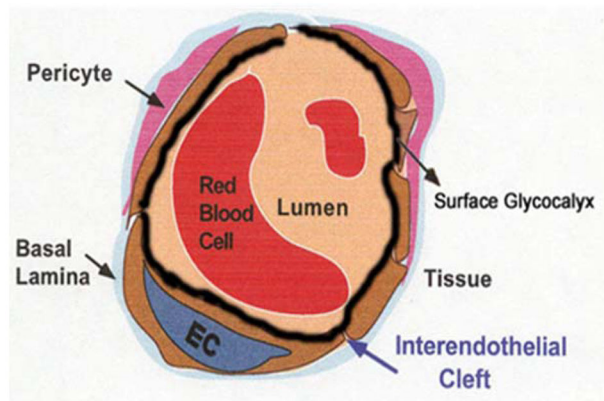
34. Sawchuk RJ, Elmquist WF. Microdialysis in the study of drug transporters in the CNS. *Adv Drug Deliv Rev.* 2000; 45:295. [PubMed: 11108981]
35. Kay GG. The effects of antihistamines on cognition and performance. *J Allergy Clin Immunol.* 2000; 105:S622. [PubMed: 10856168]
36. Schuetz EG, Schinkel AH, Relling MV, Schuetz JD. P-glycoprotein: a major determinant of rifampicin-inducible expression of cytochrome P4503A in mice and humans. *Proc Natl Acad Sci U S A.* 1996; 93:4001. [PubMed: 8633005]
37. Begley, DJ. *Enhancement in Drug Delivery.* Vol. 575. CRC Press; Boca Raton: 2007. Structure and function of the blood-brain barrier.
38. Shimizu S. A novel approach to the diagnosis and management of meralgia paresthetica. *Neurosurgery.* 2008; 63(4):E820.
39. Wolburg-Buchholz K, Mack AF, Steiner E, Pfeiffer F, Engelhardt B, Wolburg H. Loss of astrocyte polarity marks blood-brain barrier impairment during experimental autoimmune encephalomyelitis. *Acta Neuropathol.* 2009; 18(2):219.
40. Li G, Yuan W, Fu BM. A Model for Water and Solute Transport across the Blood-Brain Barrier. *J of Biomechanics.* 2010; 43(11):2133.
41. Curry, FE. The cardiovascular system. The American Physiology Society; Bethesda: 1983. Mechanics and thermodynamics of transcapillary exchange. *Handbook of Physiology.*
42. Cornford EM, Young D, Paxton JW, Sofia RD. Blood-brain barrier penetration of felbamate. *Epilepsia.* 1992; 33:944. [PubMed: 1396440]
43. van Uitert RL, Sage JI, Levy DE, Duffy TE. Comparison of radio-labeled butanol and iodoantipyrine as cerebral blood flow markers. *Brain Res.* 1981; 222:365. [PubMed: 7284784]
44. Zlokovic BV, Begley DJ, Djuricic BM, Mitrovic DM. Measurement of solute transport across the blood-brain barrier in the perfused guinea pig brain: method and application to N-methyl-alpha-aminoisobutyric acid. *J Neurochem.* 1986; 46:1444. [PubMed: 3083044]
45. de Lange EC, de Boer BA, Breimer DD. Microdialysis for pharmacokinetic analysis of drug transport to the brain. *Adv Drug Deliv Rev.* 1999; 36:211. [PubMed: 10837717]
46. Elsinga PH, Hendrikse NH, Bart J, Vaalburg W, van Waarde A. PET Studies on P-glycoprotein function in the blood-brain barrier: how it affects uptake and binding of drugs within the CNS. *Curr Pharm Des.* 2004; 10:1493. [PubMed: 15134571]
47. Wang R, Ashwal S, Tone B, Tian HR, Badaut J, Rasmussen A, Obenaus A. Albumin reduces blood-brain barrier permeability but does not alter infarct size in a rat model of neonatal stroke. *Pediatr Res.* 2007; 62:261. [PubMed: 17622953]
48. Gaber MW, Yuan H, Killmar JT, Naimark MD, Kiani MF, Merchant TE. An intravital microscopy study of radiation-induced changes in permeability and leukocyte-endothelial cell interactions in the microvessels of the rat pia mater and cremaster muscle. *Brain Res Protoc.* 2004; 13:1.
49. Easton AS, Fraser PA. Variable restriction of albumin diffusion across inflamed cerebral microvessels of the anaesthetized rat. *J Physiol.* 1994; 475:147. [PubMed: 8189387]
50. Yuan W, Lv Y, Zeng M, Fu BM. Non-invasive measurement of solute permeability in cerebral microvessels of the rat. *Microvasc Res.* 2009; 77:166. [PubMed: 18838082]
51. Nicolazzo JA, Charman SA, Charman WN. Methods to assess drug permeability across the blood-brain barrier. *J Pharm Pharmacol.* 2006; 58:281. [PubMed: 16536894]
52. Allt G, Lawrenson JG. Is the pial microvessel a good model for blood-brain barrier studies? *Brain Research Reviews.* 1997; 24:67. [PubMed: 9233542]
53. Easton AS, Sarker MH, Fraser PA. Two components of blood-brain barrier disruption in the rat. *J Physiol.* 1997; 503(3):613. [PubMed: 9379415]
54. Fu BM, Shen S. Acute VEGF effect on solute permeability of mammalian microvessels in vivo. *Microvasc Res.* 2004; 68:51. [PubMed: 15219420]
55. Franke H, Galla HJ, Beuckmann CT. An improved low-permeability in vitro-model of the blood-brain barrier: transport studies on retinoids, sucrose, haloperidol, caffeine and mannitol. *Brain Research.* 1999; 818(1):65. [PubMed: 9914438]

56. Meyer J, Mischeck U, Veyhl M, Henzel K, Galla HJ. Blood-brain barrier characteristic enzymatic properties in cultured brain capillary endothelial cells. *Brain Res.* 1990; 514(2):305. [PubMed: 1972640]
57. Hemmila JM, Drewes LR. Glucose transporter (GLUT1) expression by canine brain microvessel endothelial cells in culture: an immunocytochemical study. *Adv Exp Med Biol.* 1993; 331:13. [PubMed: 8333327]
58. Abbott NJ. Astrocyte-endothelial interactions and blood-brain barrier permeability. *Journal of Anatomy.* 2002; 200(6):629. [PubMed: 12162730]
59. Haseloff RF, Blasig IE, Bauer HC, Bauer H. In search of the astrocytic factor(s) modulating blood-brain barrier functions in brain capillary endothelial cells in vitro. *Cell Mol Neurobiol.* 2005; 25(1):25. [PubMed: 15962507]
60. Gaillard PJ, de Boer AG. Relationship between permeability status of the blood-brain barrier and in vitro permeability coefficient of a drug. *European Journal of Pharmaceutical Sciences.* 2000; 12(2):95. [PubMed: 11102736]
61. Demeuse P, Kerkhofs A, Struys-Ponsar C, Knoops B, Remacle C, de Aguilar PV. Compartmentalized coculture of rat brain endothelial cells and astrocytes: a syngenic model to study the blood-brain barrier. *Journal of Neuroscience Methods.* 2002; 121(1):21. [PubMed: 12393158]
62. Deli MA, Abraham CS, Kataoka Y, Niwa M. Permeability studies on in vitro blood-brain barrier models: Physiology, pathology, and pharmacology. *Cellular and Molecular Neurobiology.* 2005; 25(1):59. [PubMed: 15962509]
63. Brown RC, Morris AP, O'Neil RG. Tight junction protein expression and barrier properties of immortalized mouse brain microvessel endothelial cells. *Brain Res.* 2007; 1130(1):17. [PubMed: 17169347]
64. Soga N, Connolly JO, Chellaiah M, Kawamura J, Hruska KA. Rac regulates vascular endothelial growth factor stimulated motility. *Cell Commun Adhes.* 2001; 8(1):1. [PubMed: 11775025]
65. Yoder EJ. Modifications in astrocyte morphology and calcium signaling induced by a brain capillary endothelial cell line. *Glia.* 2002; 38(2):137. [PubMed: 11948807]
66. Yuan W, Li G, Fu BM. Effect of Surface Charge of Immortalized Mouse Cerebral Endothelial Cell Monolayer on Transport of Charged Solutes. *Annals of Biomedical Engineering.* 2010; 38(4): 1463. [PubMed: 20087768]
67. Tyagi N, Moshal KS, Sen U, Vacek TP, Kumar M, Hughes WM Jr, Kundu S, Tyagi SC. H2S protects against methionine-induced oxidative stress in brain endothelial cells. *Antioxid Redox Signal.* 2009; 11(1):25. [PubMed: 18837652]
68. Omidi Y, Campbell L, Barar J, Connell D, Akhtar S, Gumbleton M. Evaluation of the immortalised mouse brain capillary endothelial cell line, bEnd3, as an in vitro blood-brain barrier model for drug uptake and transport studies. *Brain Res.* 2003; 990(1-2):95. [PubMed: 14568334]
69. Malina KC, Cooper I, Teichberg VI. Closing the gap between the in-vivo and in-vitro blood-brain barrier tightness. *Brain Res.* 2009; 1284:12. [PubMed: 19501061]
70. Bowman PD, Ennis SR, Rarey KE, Betz AL, Goldstein GW. Brain microvessel endothelial cells in tissue culture: a model for study of blood-brain barrier permeability. *Ann Neurol.* 1983; 14(4):396. [PubMed: 6638956]
71. Thompson SE, Cavitt J, Audus KL. Leucine-Enkephalin Effects on Paracellular and Transcellular Permeation Pathways across Brain Microvessel Endothelial-Cell Monolayers. *Journal of Cardiovascular Pharmacology.* 1994; 24(5):818. [PubMed: 7532761]
72. Salvetti F, Cecchetti P, Janigro D, Lucacchini A, Benzi L, Martini C. Insulin permeability across an in vitro dynamic model of endothelium. *Pharmaceutical Research.* 2002; 19(4):445. [PubMed: 12033378]
73. Karyekar CS, Fasano A, Raje S, Lu RL, Dowling TC, Eddington ND. Zonula occludens toxin increases the permeability of molecular weight markers and chemotherapeutic agents across the bovine brain microvessel endothelial cells. *Journal of Pharmaceutical Sciences.* 2003; 92(2):414. [PubMed: 12532391]
74. Hamm S, Dehouck B, Kraus J, Wolburg-Buchholz K, Wolburg H, Risau W, Cecchelli R, Engelhardt B, Dehouck MP. Astrocyte mediated modulation of blood-brain barrier permeability

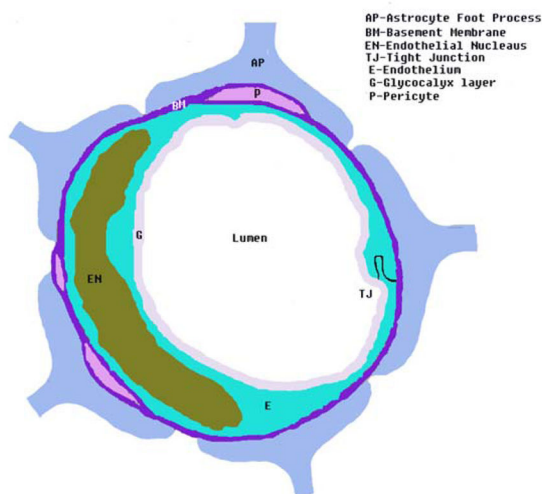
- does not correlate with a loss of tight junction proteins from the cellular contacts. *Cell and Tissue Research*. 2004; 315(2):157. [PubMed: 14615934]
75. Kemper EM, Boogerd W, Thuis I, Beijnen JH, van Tellingen O. Modulation of the blood-brain barrier in oncology: therapeutic opportunities for the treatment of brain tumours? *Cancer Treatment Reviews*. 2004; 30(5):415. [PubMed: 15245774]
76. Boveri M, Berezowski V, Price A, Slupek S, Lenfant AM, Benaud C, Hartung T, Cecchelli R, Prieto P, Dehouck MP. Induction of blood-brain barrier properties in cultured brain capillary endothelial cells: Comparison between primary glial cells and C6 cell line. *Glia*. 2005; 51(3):187. [PubMed: 15800928]
77. Kraus J, Voigt K, Schuller AM, Scholz M, Kim KS, Schilling M, Schabitz WR, Oschmann P, Engelhardt B. Interferon-beta stabilizes barrier characteristics of the blood-brain barrier in four different species in vitro. *Multiple Sclerosis*. 2008; 14(6):843. [PubMed: 18505778]
78. Poller B, Gutmann H, Krahenbuhl S, Weksler B, Romero I, Couraud PO, Tuffin G, Drewe J, Huwyler J. The human brain endothelial cell line hCMEC/D3 as a human blood-brain barrier model for drug transport studies. *Journal of Neurochemistry*. 2008; 107(5):1358. [PubMed: 19013850]
79. Sahagun G, Moore SA, Hart MN. Permeability of neutral vs. anionic dextrans in cultured brain microvascular endothelium. *Am J Physiol*. 1990; 259(1 Pt 2):H162. [PubMed: 1695819]
80. Santaguida S, Janigro D, Hossain M, Oby E, Rapp E, Cucullo L. Side by side comparison between dynamic versus static models of blood-brain barrier in vitro: A permeability study. *Brain Research*. 2006; 1109:1. [PubMed: 16857178]
81. de Vries HE, BlomRoosemalen MCM, van Oosten M, de Boer AG, van Berkel TJ, Breimer DD, Kuiper J. The influence of cytokines on the integrity of the blood-brain barrier in vitro. *Journal of Neuroimmunology*. 1996; 64(1):37. [PubMed: 8598388]
82. Cucullo L, McAllister MS, Kight K, Krizanac-Bengez L, Marroni M, Mayberg MR, Stanness KA, Janigro D. A new dynamic in vitro model for the multidimensional study of astrocyte-endothelial cell interactions at the blood-brain barrier. *Brain Research*. 2002; 951(2):243. [PubMed: 12270503]
83. Zhang Y, Li CS, Ye YY, Johnson K, Poe J, Johnson S, Bobrowski W, Garrido R, Madhu C. Porcine brain microvessel endothelial cells as an in vitro model to predict in vivo blood-brain barrier permeability. *Drug Metabolism and Disposition*. 2006; 34(11):1935. [PubMed: 16896068]
84. Li G, Simon M, Shi Z, Cancel L, Tarbell JM, Morrison B, Fu BM. Permeability of endothelial and astrocyte cocultures: in vitro blood-brain barrier models for drug delivery. *Ann of Biomed Eng*. 2010; 38(8):2499. [PubMed: 20361260]
85. Engvall E. Structure and function of basement membranes. *Int J Dev Biol*. 1995; 39(5):781. [PubMed: 8645562]
86. Miosge N. The ultrastructural composition of basement membranes in vivo. *Histol Histopathol*. 2001; 16(4):1239. [PubMed: 11642743]
87. Kleinman HK, Martin GR. Matrigel: basement membrane matrix with biological activity. *Semin Cancer Biol*. 2005; 15(5):378. [PubMed: 15975825]
88. Pardridge WM. Molecular biology of the blood-brain barrier. *Molecular Biotechnology*. 2005; 30(1):57. [PubMed: 15805577]
89. Dietrich WD, Alonso O, Halley M. Early microvascular and neuronal consequences of traumatic brain injury: a light and electron microscopic study in rats. *J Neurotrauma*. 1994; 11(3):289. [PubMed: 7996583]
90. Fukuda K, Tanno H, Okimura Y, Nakamura M, Yamaura A. The blood-brain barrier disruption to circulating proteins in the early period after fluid percussion brain injury in rats. *J Neurotrauma*. 1995; 12(3):315. [PubMed: 7473806]
91. Baldwin SA, Fugaccia I, Brown DR, Brown LV, Scheff SW. Blood-brain barrier breach following cortical contusion in the rat. *J Neurosurg*. 1996; 85(3):476. [PubMed: 8751635]
92. Barzo P, Marmarou A, Fatouros P, Corwin F, Dunbar J. Magnetic resonance imaging-monitored acute blood-brain barrier changes in experimental traumatic brain injury. *J Neurosurg*. 1996; 85(6):1113. [PubMed: 8929504]

93. Baskaya MK, Rao AM, Dogan A, Donaldson D, Dempsey RJ. The biphasic opening of the blood-brain barrier in the cortex and hippocampus after traumatic brain injury in rats. *Neurosci Lett*. 1997; 226(1):33. [PubMed: 9153635]
94. Beaumont A, Marmarou A, Hayasaki K, Barzo P, Fatouros P, Corwin F, Marmarou C, Dunbar J. The permissive nature of blood brain barrier (BBB) opening in edema formation following traumatic brain injury. *Acta Neurochir Suppl*. 2000; 76:125. [PubMed: 11449990]
95. Cernak I, Vink R, Zapple DN, Cruz MI, Ahmed F, Chang T, Fricke ST, Faden AI. The pathobiology of moderate diffuse traumatic brain injury as identified using a new experimental model of injury in rats. *Neurobiol Dis*. 2004; 17(1):29. [PubMed: 15350963]
96. Fu BM, Chen B. A model for the structural mechanisms in the regulation of microvessel permeability by junction strands. *ASME J Biomech Eng*. 2003; 125:620.
97. Fu BM, Tsay R, Curry FE, Weinbaum S. A junction-orifice-entrance layer model for capillary permeability: Application to frog mesenteric capillaries. *ASME J Biomech Eng*. 1994; 116:502.
98. Schulze C, Firth JA. Interendothelial Junctions during Blood-Brain-Barrier Development in the Rat - Morphological-Changes at the Level of Individual Tight Junctional Contacts. *Developmental Brain Research*. 1992; 69(1):85. [PubMed: 1424091]
99. Adamson RH, Lenz JE, Zhang X, Adamson GN, Weinbaum S, Curry FE. Oncotic pressures opposing filtration across non-fenestrated rat microvessels. *Journal of Physiology-London*. 2004; 557:889.
100. Li G, Fu BM. An Electro-diffusion Model for the Blood-Brain Barrier Permeability to Charged Molecule. *ASME J of Biomechanical Engineering*. 2011; 133(2):0210.
101. Mak M, Fung L, Strasser JF, Saltzman WM. Distribution of drugs following controlled delivery to the brain interstitium. *J Neurooncol*. 1995; 26(2):91. [PubMed: 8787851]
102. Bobo RH, Laske DW, Akbasak A, Morrison PF, Dedrick RL, Oldfield EH. Convection-enhanced delivery of macromolecules in the brain. *Proc Natl Acad Sci U S A*. 1994; 91(6):2076. [PubMed: 8134351]
103. Kroll RA, Neuwelt EA. Outwitting the blood-brain barrier for therapeutic purposes: osmotic opening and other means. *Neurosurgery*. 1998; 42(5):1083. [PubMed: 9588554]
104. Doolittle ND, Abrey LE, Ferrari N, Hall WA, Laws ER, McLendon RE, Muldoon LL, Peereboom D, Peterson DR, Reynolds CP, Senter P, Neuwelt EA. Targeted delivery in primary and metastatic brain tumors: summary report of the seventh annual meeting of the Blood-Brain Barrier Disruption Consortium. *Clin Cancer Res*. 2002; 8(6):1702. [PubMed: 12060607]
105. Hynynen K, McDannold N, Vykhodtseva N, Jolesz FA. Noninvasive MR imaging-guided focal opening of the blood-brain barrier in rabbits. *Radiology*. 2001; 220(3):640. [PubMed: 11526261]
106. Hynynen K, McDannold N, Vykhodtseva N, Raymond S, Weissleder R, Jolesz FA, Sheikov N. Focal disruption of the blood-brain barrier due to 260-kHz ultrasound bursts: a method for molecular imaging and targeted drug delivery. *J Neurosurg*. 2006; 105(3):445. [PubMed: 16961141]
107. Kinoshita M. Targeted drug delivery to the brain using focused ultrasound. *Top Magn Reson Imaging*. 2006; 17(3):209. [PubMed: 17414078]
108. Dean RL, Emerich DF, Hasler BP, Bartus RT. Cereport (RMP-7) increases carboplatin levels in brain tumors after pretreatment with dexamethasone. *Neuro Oncol*. 1999; 1(4):268. [PubMed: 11550318]
109. Borlongan CV, Emerich DF. Facilitation of drug entry into the CNS via transient permeation of blood brain barrier: laboratory and preliminary clinical evidence from bradykinin receptor agonist, Cereport. *Brain Res Bull*. 2003; 60(3):297. [PubMed: 12754091]
110. Gabathuler R. Approaches to transport therapeutic drugs across the blood-brain barrier to treat brain diseases. *Neurobiol Dis*. 2010; 37(1):48. [PubMed: 19664710]
111. Lipinski CA. Drug-like properties and the causes of poor solubility and poor permeability. *J Pharmacol Toxicol Methods*. 2000; 44(1):235. [PubMed: 11274893]
112. Shashoua VE, Hesse GW. N-docosahexaenoyl, 3 hydroxytyramine: a dopaminergic compound that penetrates the blood-brain barrier and suppresses appetite. *Life Sci*. 1996; 58(16):1347. [PubMed: 8614292]

113. Sawada GA, Williams LR, Lutzke BS, Raub TJ. Novel, highly lipophilic antioxidants readily diffuse across the blood-brain barrier and access intracellular sites. *J Pharmacol Exp Ther.* 1999; 288(3):1327. [PubMed: 10027874]
114. Bodor N, Farag HH, Brewster ME. Site-specific, sustained release of drugs to the brain. *Science.* 1981; 214(4527):1370. [PubMed: 7313698]
115. Brewster ME, Raghavan K, Pop E, Bodor N. Enhanced delivery of ganciclovir to the brain through the use of redox targeting. *Antimicrob Agents Chemother.* 1994; 38(4):817. [PubMed: 8031052]
116. Pardridge WM. Blood-brain barrier drug targeting: the future of brain drug development. *Mol Interv.* 2003; 3(2):90. [PubMed: 14993430]
117. Pardridge WM. Molecular Trojan horses for blood-brain barrier drug delivery. *Curr Opin in Pharm.* 2006; 6(5):494.
118. Miller G. Drug targeting. Breaking down barriers *Science.* 2002; 297(5584):1116. [PubMed: 12183610]
119. Gosk S, Vermehren C, Storm G, Moos T. Targeting anti-transferrin receptor antibody (OX26) and OX26-conjugated liposomes to brain capillary endothelial cells using in situ perfusion. *J Cereb Blood Flow Metab.* 2004; 24(11):1193. [PubMed: 15545912]
120. Kumagai AK, Eisenberg JB, Pardridge WM. Adsorptive-mediated endocytosis of cationized albumin and a beta-endorphin-cationized albumin chimeric peptide by isolated brain capillaries. Model system of blood-brain barrier transport. *J Biol Chem.* 1987; 262(31):15214. [PubMed: 2959663]
121. Lawrenson JG, Reid AR, Allt G. Molecular characteristics of pial microvessels of the rat optic nerve. Can pial microvessels be used as a model for the blood-brain barrier? *Cell Tissue Res.* 1997; 288:259–65. [PubMed: 9082961]
122. Yuan W, Li G, Zeng M, Fu BM. Modulation of the Blood-brain barrier permeability by plasma glycoprotein orosomucoid. *Microvasc Res.* 2010; 80(1):148–157. [PubMed: 20362593]
123. Hervé F, Ghinea N, Scherrmann JM. CNS delivery via adsorptive transcytosis. *AAPS J.* 2008; 10(3):455. [PubMed: 18726697]
124. Rousselle C, Clair P, Smirnova M, Kolesnikov Y, Pasternak GW, Gac-Breton S, Rees AR, Scherrmann JM, Temsamani J. Improved brain uptake and pharmacological activity of dalargin using a peptide-vector-mediated strategy. *J Pharmacol Exp Ther.* 2003; 306(1):371. [PubMed: 12682214]
125. Liu L, Guo K, Lu J, Venkatraman SS, Luo D, Ng KC, Ling EA, Moochhala S, Yang YY. Biologically active core/shell nanoparticles self-assembled from cholesterol-terminated PEG-TAT for drug delivery across the blood-brain barrier. *Biomaterials.* 2008; 29(10):1509. [PubMed: 18155137]
126. Lockman PR, Koziara JM, Mumper RJ, Allen DD. Nanoparticle surface charges alter blood-brain barrier integrity and permeability. *J Drug Target.* 2004; 12(9–10):635. [PubMed: 15621689]



(a)



(b)

Figure 1. Schematic of the cross-sectional view of: (a) a peripheral microvessel (the microvessel in non-brain organs), and (b) the blood-brain barrier (BBB) or cerebral microvessel (the microvessel in the brain). In addition to other structures as in a peripheral microvessel, the BBB is wrapped by astrocyte foot processes (AP). BM, Basement membrane (or basal lamina); E, endothelial cell; EN, nucleus of endothelial cell; P, pericytes; G, surface glyocalyx layer; TJ, tight junction. Modified from [40].

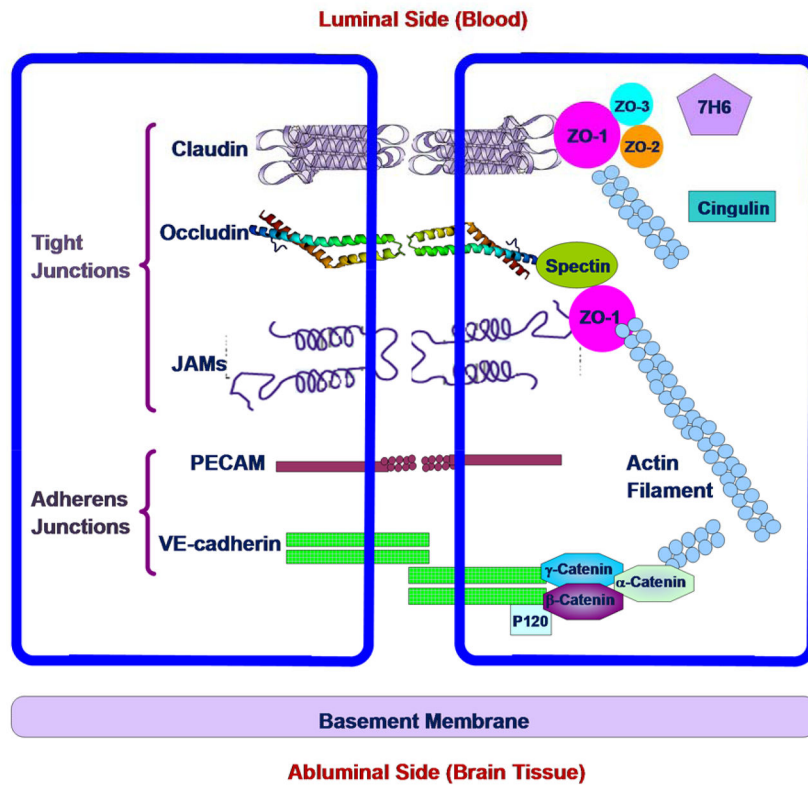


Figure 2. Schematic of junctional complex in the paracellular pathway of the BBB. Modified from [27, 28].

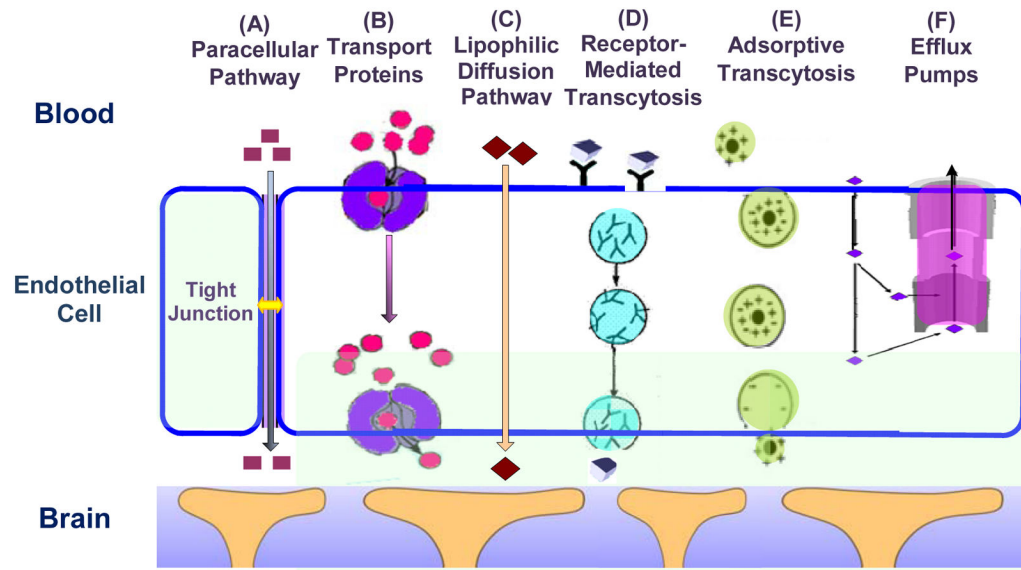


Figure 3. Transport pathways across the brain endothelial cell. Modified from [33].

Author Manuscript

Author Manuscript

Author Manuscript

Author Manuscript

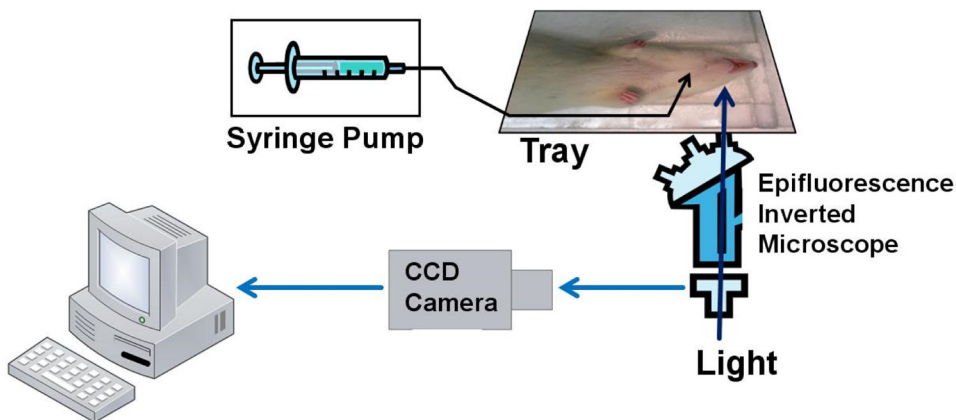


Figure 4. Schematic for the *in vivo* permeability measurement of rat cerebral microvessels. The fluorescence solution was injected into the brain via a carotid artery with a syringe pump. The fluorescence images were captured by a CCD camera, which was connected to an inverted microscope. The image analysis software was then used to measure the fluorescence intensity for the region of interest in each image.

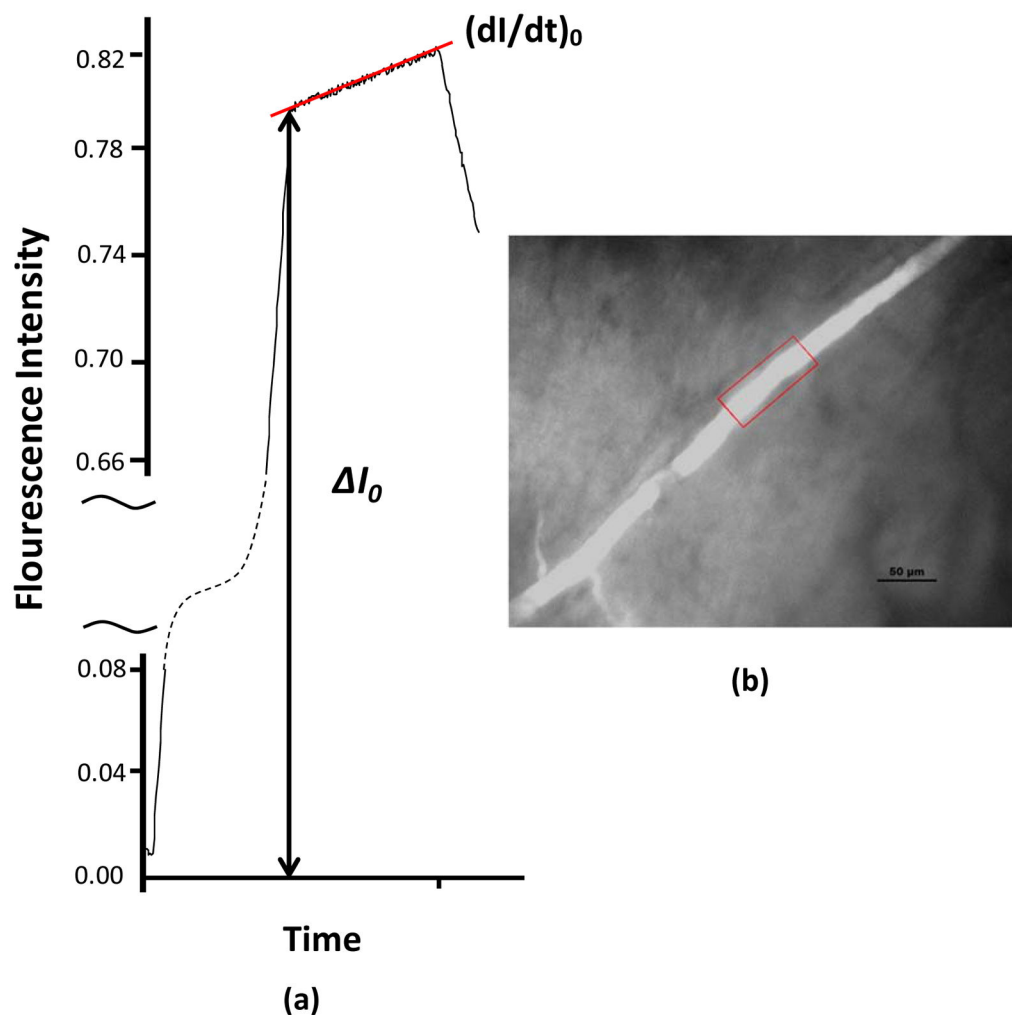


Figure 5. Quantitative fluorescence imaging method for the measurement of solute permeability in a rat pial microvessel. The images were collected during the *in vivo* experiments and the fluorescence intensity was analyzed off-line. When the fluorescence labeled test solute was injected into the carotid artery, the pial microvessel lumen filled with fluorescent solute (red frame in **b**), producing I_0 . With continued perfusion, the measured fluorescence intensity increased indicating further transport of the solute out of the microvessel and into the surrounding tissue. The initial solute flux into the tissue was measured from the slope $(dI/dt)_0$ (**a**). The solute permeability P was calculated by $P = 1/ I_0 (dI/dt)_0 r/2$. Here r is the microvessel radius. Redrawn from [50]. The scale bar in (**b**) is $50 \mu\text{m}$.

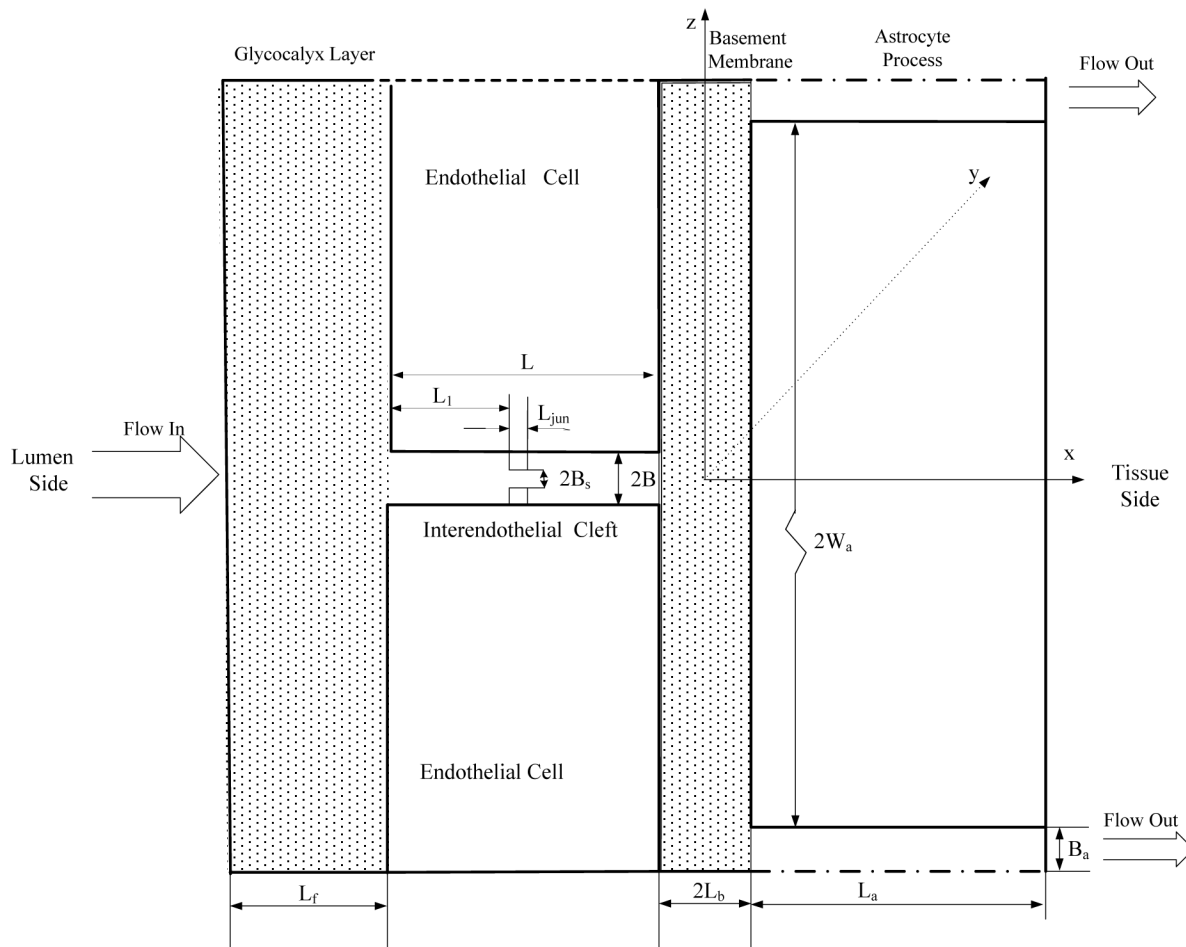
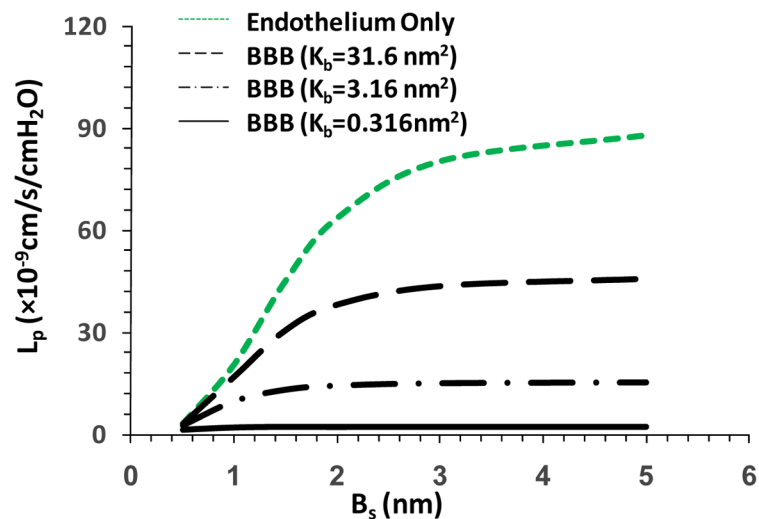
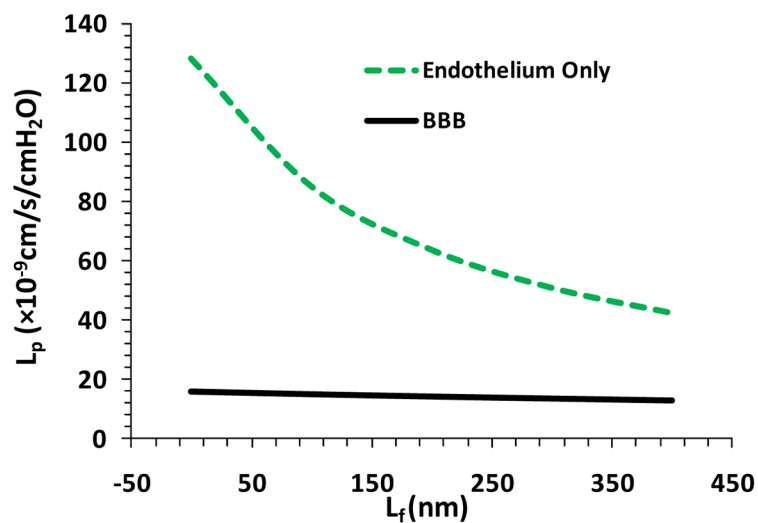


Figure 6.

Model geometry for the paracellular pathway of the BBB (Not in scale). The thickness of the endothelial surface glycocalyx layer is L_f . The inter-endothelial cleft has a length of L and a width of $2B$. The length of the tight junction strand in the inter-endothelial cleft is L_{jun} . The width of the small continuous slit in the junction strand is $2B_s$. The distance between the junction strand and luminal front of the cleft is L_1 . The width of the basement membrane is $2L_b$ and the length of the astrocyte foot processes is $2W_a$. The cleft between astrocyte foot processes has a length of L_a and a width of $2B_a$. The surface glycocalyx layer and the endothelial cells are defined as the Endothelium only while the BBB is defined to include the endothelium, the basement membrane and the astrocytes. Redrawn from [40].



(a)



(b)

Figure 7.

Model predictions for hydraulic conductivity L_p (a) as a function of B_s , the half width of the small slit in the junction strand under two cases: when considering transport across the endothelium only (Endothelium only, green line), and when considering transport across the entire BBB (BBB). In the BBB case, three different fiber densities were considered for the basement membrane: the same as the fiber density in the surface glycocalyx layer ($K_b=3.16\text{cm}^2$, the dash-dot-dash line), ten times lower ($K_b=31.6\text{cm}^2$, the dashed line) and higher ($K_b=0.316\text{cm}^2$, the solid line); (b) as a function of the surface glycocalyx layer thickness L_f . Redrawn from [40].